CJC Chinese Journal of Chemistry 中国化学 - An International Journal

For submission: https://mc.manuscriptcentral.com/cjoc
For published articles: https://onlinelibrary.wiley.com/journal/16147065

Concise Report

Cite this paper: *Chin. J. Chem.* **2021**, *39*, 1093—1103. **DOI: 10.1002/cjoc.202000627**

Synthesis and Biological Evaluation of Quinazolonethiazoles as New Potential Conquerors towards *Pseudomonas Aeruginosa*

Jie Wang, Narsaiah Battini, Mohammad Fawad Ansari, and Cheng-He Zhou*

Institute of Bioorganic & Medicinal Chemistry, Key Laboratory of Luminescence Analysis and Molecular Sensing (Southwest University), Ministry of Education, School of Chemistry and Chemical Engineering, Southwest University, Chongqing 400715, China

Keywords

Thiazole | Schiff bases | Antimicrobial | Drug design | DNA

Main observation and conclusion

Novel quinazolonthiazoles were designed and synthesized as new potential antimicrobial agents by facile multi-step procedure from *o*-aminobenzoic acids and 2-acetylthiazole. A series of biological evaluation showed that compound **7d** was the most effective quinazolonethiazole with superior activity to reference drugs chloramphenicol and norfloxacin. This active molecule displayed unobvious bacterial resistance against *P. aeruginosa*, the low toxicity to normal hepatocytes, suitable pharmacokinetics and drug-likeness. The preliminary biological interaction suggested that quinazolonethiazole **7d** might induce bacterial death by disturbing the membrane permeability, whilst preventing bacteria from growth by integrating into DNA and binding with topoisomerase IV. These findings provided significant background for the further development of quinazolonethiazoles as new potential drugs in combating drug-resistant pathogens.

Comprehensive Graphic Content

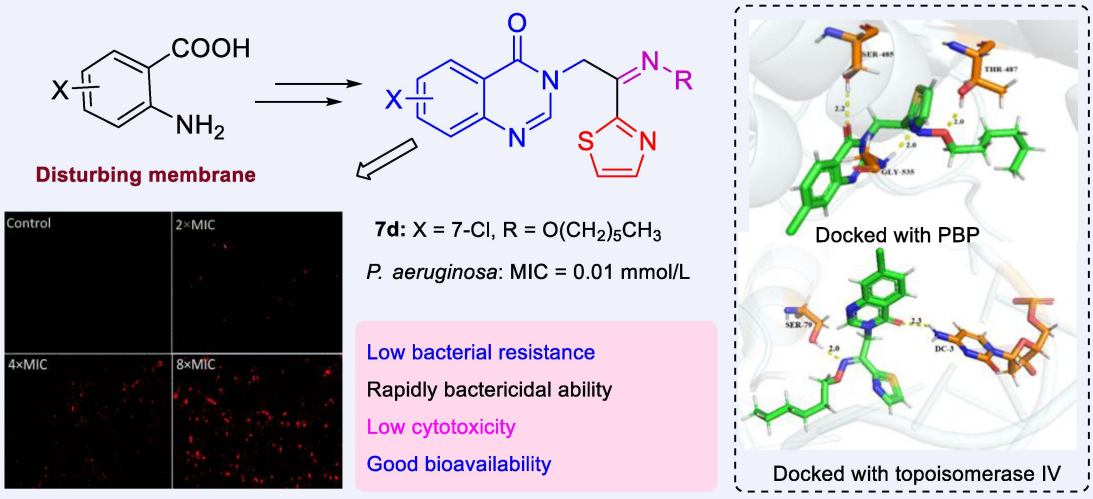

*E-mail: zhouch@swu.edu.cn

View HTML Article | Supporting Information

Background and Originality Content

The alarmingly escalating microbial resistance continues to threaten the longevity and effectiveness of available antibiotics, causing the increased mortality of infected patients and aggravating the clinical challenge of tackling infections,[1] which could accelerate the process of approaching post-antibiotic era.[2] Accordingly, the research of novel antimicrobials is an immediate matter for discovery of new medicinal drugs to address causative diseases.

Quinazolone widely exists in many bioactive agents including naturally occurring alkaloids and synthetic compounds.[3-4] The unique structural feature of quinazolone backbone is identified as a new and important chemical structural framework, naturally its derivatives tremendously captivate attention on the synthesis, structural modification and biomedical effects.[5] Especially for the antibacterial properties, quinazolone does not contain β-lactam ring but exerts the similar mechanism of action to ceftaroline that could bind to the allosteric site of penicillin-binding protein (PBP).[6] More relevantly, quinazolone with benzopyrimidone skeleton is structurally different from the C-3 position at quinolone having benzopyridone core (Figure 1), and some studies revealed that the drug resistance of quinolones is primarily associated with the chelation of the carboxyl group at C-3 position.[7] These significant properties suggest that quinazolones could have potential to replace quinolones in exerting similar biological efficacy against drug-resistant strains.[8] In fact, some reported quinazolones showed higher activity than clinical drugs against dreadful pathogens.[9] Therefore, a promising approach to overcome resistance problem might be to develop innovative quinazolones by modifying the 3-position of quinazolones. This type of new derivatives maybe exert multiple modes of action.

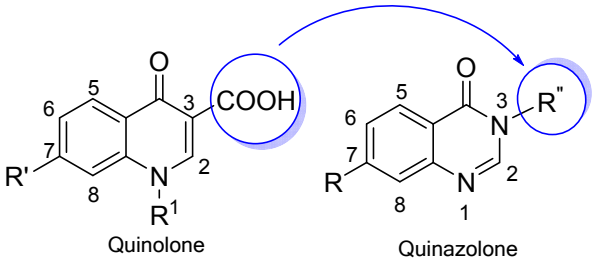

Figure 1 The main structures of quinolone and quinazolone.

The five-member aromatic heterocyclic thiazole has been well-known for valuable contributions to the efficacy of clinically available antimicrobial drugs,[10] such as antibacterial ceftaroline fosamil acetate and aztreonam, antifungal ravuconazole and abafungin.[11] This could be attributed to the unique structure of thiazole ring with both electron-donating groups (NH or S) and electron-withdrawing group (C=N), which endows it to have the multi-binding ability to functional targets through diverse weak interactions.[12-13] The successful exploitation of numerous thiazole-based medications has been stimulating immense efforts to develop the conjugates of thiazole with various pharmacophores. This conjugation strategy has occupied a prominent place in discovery of new bioactive species.[14-15] Recently, the incorporation of thiazole ring into the antibacterial quinolone skeleton not only facilitates conjugates to possess the excellent bioactivities but also affects bacterial cellular normal processes including membrane permeability and DNA replication.[16] Thus, the introduction of thiazole in the C-3 position at quinazolone might construct more effective antimicrobial candidates.

Imine is a helpful functional group in exerting bioactivity because it easily performs hydrogen bonds, coordination and/or polar interactions to regulate the lipid-water partition and to improve pharmacokinetics and biocompatibility, thereby presenting in the majority of drugs.[17-18] Particularly, many antibacterial drugs containing thiazole ring usually have the presence of imine bond like cefixime and cefdinir,[19-20] and extensive work has been devoted to the introduction of imine in the development of antimicrobials about quinazolone,[21] most of which display excellent antimicrobial activity.[22] This might mean that imine fragment is extremely important for the biological activity of compounds like thiazoles and quinazolones. As a result, these stimulating properties promote the synthesis of thiazole conjugated quinazolinone with different imine moieties including oximes, hydrazines and methylenimines for antimicrobials development.

In present work, the thiazole conjugated quinazolones as novel potential antimicrobial hybrids were designed and synthesized against bacterial and fungal strains with the hope of high safety, low microbial resistance and good bioavailability (Figure 2). For purpose of verifying the research value of this framework, the experiments involving bacterial resistance study, bactericidal kinetic study, cytotoxicity and ADME study were performed. In addition, antibacterial mechanisms including biofilm destruction, molecular docking study and the interaction with DNA were preliminarily explored to correlate them with their antimicrobial activities. This series of studies might provide valuable information for the design of new antimicrobial analogues with improved activity.

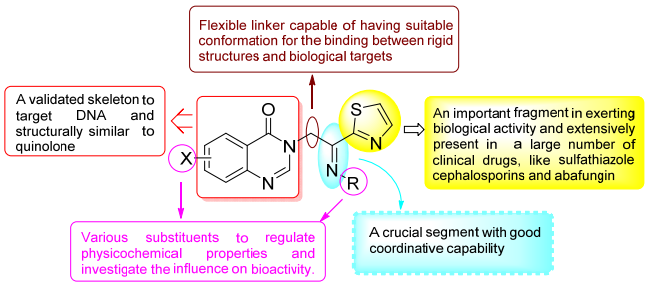

Figure 2 Design of novel structural potential antimicrobial target quinazolonethiazoles.

Results and Discussion

Chemistry

The preparation of target quinazolonethiazoles was carried out according to Scheme 1. The commercially available formamidine acetate and anthranilic acid with different substituents were used as starting materials to construct quinazolone skeleton **2**. Bromination of 2-acetylthiazole **8** gave 2-bromoacetylthiazole **9**, which was coupled with quinazolone skeleton **2** to afford the important precursors **3a**—**3d** with yields of 25.2%—49.9% in presence of potassium carbonate. Experiments revealed that quinazolones with electron-donating groups could not successfully react with 2-bromoacetylthiazole **9**, which may be attributed to the influences of electron density on reactivity of quinazolones, and the yield increased as the electron density in quinazolones decreased. The condensation reaction of compound **3a** with different primary amines resulted in the formation of methylenimine derivations **4a**—**4e** in yields of 32.8%—58.0% using acetic acid as catalyst and ethanol as solvent. Under similar conditions, hydrazone compounds **5a**—**5e** in good yields of 56.3%—82.7% were easily produced by reacting **3a** with different hydrazines. Moreover, the precursor **3a** was treated with hydroxylamine hydrochloride to furnish the oxime **6**, which was further modified by introducing alkyl halides at the *O*-atom of the oxime group in acetonitrile to produce the oxime derivatives **7a**—**7g** in

Scheme 1 Preparative process of target quinazolonethiazoles

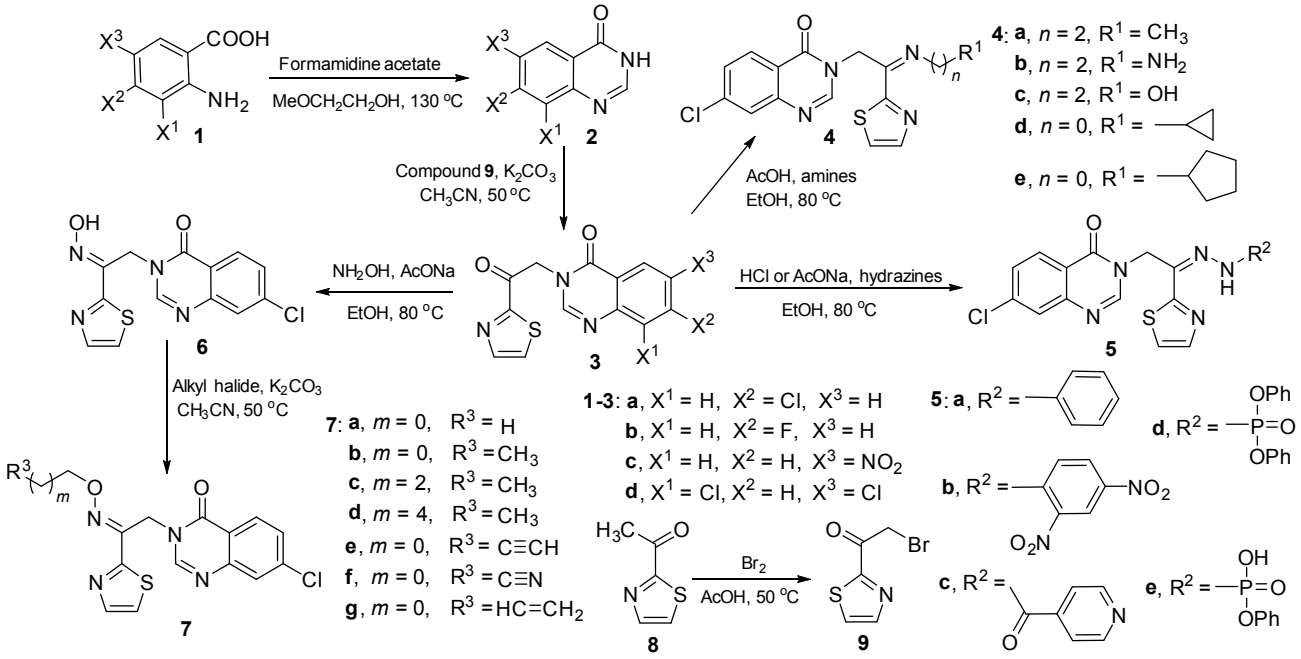

yields ranging from 45.8% to 79.7%.

Analysis of configuration (*E* or *Z*)

The carbonyl group of quinazolonethiazole **3a** was condensed with the primary amine to form target imines **4a**—**4e** and **5a**—**5e** as well as oxime **6**. Theoretically, there should be two configurations for tautomeric equilibrium. Thus, the single crystal of hydrazone derivative **5d** was further cultured in order to understand its structure. X-ray diffraction analysis pointed out that the obtained single crystal of hydrazone derivative **5d** (Figure 3) showed the *Z* configuration, which could be ascribed to that the *E* configuration is general instability or easy conversion to the *Z* configuration.

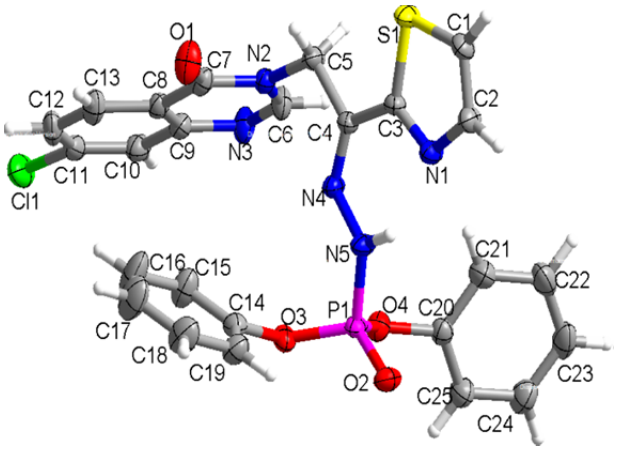

Figure 3 Crystal structure of quinazolonethiazole **5d**.

Antibacterial activity

To elucidate the structures of novel quinazolonethiazoles on effects of antimicrobial activity, the antibacterial evaluations were operated and the results were shown in Table 1. The first prepared quinazolonethiazoles **3a**—**3d** with different substituents on the benzene ring showed moderate antibacterial activity. In particular, compound **3a** containing chlorine substitution not only exhibited stronger anti-*E. faecalis* effect (MIC = 0.01 mmol/L) than reference drugs chloramphenicol and norfloxacin, but also gave excellent antibacterial activity against Gram-positive stain *S. aureus* ATCC 29213 with MIC value of 0.003 mmol/L, which was 3-fold and 8-fold more potent than the clinical antibacterial chloramphenicol (MIC = 0.01 mmol/L) and norfloxacin (MIC = 0.025 mmol/L), respectively. Therefore, the structural modification of compound **3a** was carried out to construct novel quinazolonethiazole imines. The quinazolone thiazoles with methylenimines **4a**—**4e** showed moderate or weak biological activity with MIC values in the range of 0.05—0.74 mmol/L in comparison with reference drugs. However, they showed superior inhibition efficacy to precursor **3a** for most of the tested bacterial strains, especially aminoethyl and hydroxyethyl modified Schiff bases **4b** and **4c**, which were far stronger than compound **3a** (MIC = 0.84 mmol/L) towards drug-resistant *S. aureus* having MIC values of 0.05 mmol/L. The above information pointed out that the introduction of Schiff base on compound **3a** occupied a prominent place on antibacterial activity.

To better analyze the structure-activity relationship (SAR) and enrich the structural diversity, imine compounds **4b**—**4c** with the best activity were further modified to yield hydrazones **5a**—**5e** and oximes **7a**—**7g**. As for hydrazone-derived quinazolonethiazoles **5a**—**5e**, the antibacterial activities did not exhibit significant improvement in comparison to aminoethyl derivative **4b**, except for compound **5d**, which could inhibit the growth of MRSA and *E. faecalis* with a little lower MIC value of 0.06 mmol/L. For another, hexyl oxime derivative **7d** not only displayed good inhibitory activities against tested strains, but also was more effective than chloramphenicol and norfloxacin against the growth of *P. aeruginosa* and *P. aeruginosa* ATCC 27853, while the other oxime compounds including unsaturated alkyl chain apparently lost bioactivity compared to compound **7d**. However, in general, the introduction of oxime fragment was beneficial to antibacterial activity.

Antifungal activity

The *in vitro* antifungal results in Table S1 showed that the inhibitory activities of the target compounds were generally inferior to that of fluconazole against the tested fungi apart from *A. fumigatus.* The antifungal activities of precursor **3a** showed twice

Table 1 *In vitro* antibacterial data as MIC (mmol/L) for quinazolonethiazoles **3**—**7**[a,b]

Compds	Gram-positive bacteria[b]					Gram-negative bacteria[b]					
	MRSA	*E. f.*	*S. a.*	*S. a. 25923*	*S. a. 29213*	*K. p.*	*E. c.*	*P. a.*	*A. b.*	*P. a. 27853*	*E. c. 25922*
3a	0.21	0.01	0.84	0.84	0.003	0.84	0.84	0.84	0.84	0.84	1.67
3b	0.22	0.11	0.88	0.44	0.88	0.44	0.88	0.88	0.88	0.88	0.88
3c	0.81	0.40	0.40	0.40	0.81	0.40	0.81	0.81	0.40	0.81	0.81
3d	0.75	0.75	0.38	0.75	0.75	0.75	0.19	0.75	0.75	0.38	0.75
4a	0.74	0.37	0.74	0.74	0.19	0.74	0.74	0.74	0.74	0.74	0.37
4b	0.73	0.18	0.05	0.18	0.73	0.37	0.37	0.18	0.73	0.37	0.18
4c	0.09	0.18	0.05	0.37	0.74	0.37	0.37	0.37	0.18	0.37	0.05
4d	0.74	0.74	0.74	0.74	0.74	0.74	0.74	0.74	0.74	0.74	0.74
4e	0.69	0.34	0.69	0.34	0.69	0.69	0.69	0.69	0.69	0.69	0.69
5a	0.65	0.08	0.65	0.16	0.32	0.65	0.65	0.65	0.65	0.65	0.65
5b	0.53	0.26	0.53	0.53	0.53	0.53	0.53	0.26	0.53	0.03	0.53
5c	0.60	0.60	0.60	0.60	0.60	0.60	0.60	0.60	0.60	0.60	0.60
5d	0.06	0.06	0.46	0.46	0.23	0.23	0.23	0.46	0.46	0.46	0.46
5e	0.07	0.27	0.54	0.54	0.54	0.54	0.54	0.54	0.54	0.13	0.27
6	0.42	1.66	0.83	0.83	0.83	0.80	1.60	1.60	1.60	0.40	1.60
7a	0.38	0.19	0.76	0.38	0.76	0.38	0.38	0.76	0.76	0.19	0.76
7b	1.42	0.35	1.42	0.18	0.71	0.73	0.73	1.47	0.37	1.47	1.47
7c	0.09	0.73	0.73	0.37	0.73	0.17	0.68	1.36	0.68	0.34	0.68
7d	1.26	0.04	1.26	0.02	0.01	0.01	0.04	0.01	1.26	0.01	0.63
7e	1.60	0.80	1.60	0.40	1.60	1.43	0.71	1.43	1.43	1.43	0.71
7f	0.71	0.71	1.43	0.18	0.71	1.42	1.42	0.71	0.71	0.71	1.42
7g	0.71	1.42	1.42	0.71	1.42	0.71	1.42	0.71	1.42	1.42	1.42
A[c]	0.05	0.02	0.02	0.02	0.01	0.02	0.10	0.10	0.05	0.02	0.05
B[d]	0.003	0.013	0.006	0.013	0.025	0.002	0.001	0.025	0.006	0.025	0.050

[a] Minimal inhibitory concentrations (MIC, mmol/L) were determined by micro broth dilution method for microdilution plates. [b] MRSA, *Methicillin-Resistant Staphylococcus aureus*; *S. a.*, *Staphylococcus aureus*; *S. a.* 25923, *Staphylococcus aureus* ATCC 25923; *S. a.* 29213, *Staphylococcus aureus* ATCC 29213; *E. f.*, *Enterococcus faecalis*; *K. p.*, *Klebsiella pneumonia*; *E. c.*, *Escherichia coli*; *E. c.* 25922, *Escherichia coli* ATCC 25922; *P. a.*, *Pseudomonas aeruginosa*; *P. a.* 27853, *Pseudomonas aeruginosa* ATCC 27853; *A. b.*, *Acinetobacter baumanii*. [c] **A** = Chloramphenicol. [d] **B** = Norfloxacin.

or equal to fluconazole against *A. fumigatus* and *C. albicans* ATCC 90023, respectively. For methylenimines **4a**—**4e** and hydrazones **5a**—**5e**, they showed moderate or good inhibitory efficacy to the growth of *A. fumigatus* in comparison to molecule **3a**, and all of them were superior to the reference drug fluconazole. In addition, aminoethyl compound **4b** and hydrazone derivative **5d** displayed promising antifungal activity against *C. albicans* with MIC values of 0.09 mmol/L and 0.03 mmol/L, respectively. Noticeably, oxime **7d** displayed excellent anti-*A. fumigatus* activity with MIC value of 0.02 mmol/L, which was 42-fold more potent than fluconazole, and it also possessed better antifungal activity than precursor **3a** against all tested fungal strains, indicating that the introduction of imine was beneficial to antifungal activity.

Bactericidal kinetics

Bactericidal therapy might shorten the duration of bacterial infection and reduce the occurrence of bacterial resistant development.[23] So the bactericidal efficiency for quinazolonethiazole **7d** (6 × MIC) was evaluated by a time-kill kinetic experiment against *P. aeruginosa*, and the results (Figure 4) revealed that bacterial concentration decreased by more than 10^2 CFU/mL in presence of potent compound **7d** within 2 h, which manifested quinazolonethizole **7d** was effective in killing *P. aeruginosa*, having the possibility of alleviating bacterial resistance.

Bacterial resistance study

The frequent evolution of drug-resistant pathogens imposes restrictions on the lifespan of antibiotic, thereby limiting the curative effect of infectious diseases, so the development of drug resistance is a critical criterion for evaluating antimicrobials.[24] The bacterial resistant results (Figure 5) of quinazolonethiazole **7d**

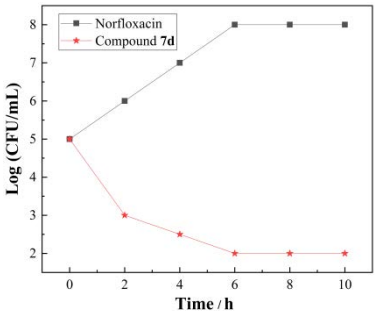

Figure 4 Time-kill kinetics of quinazolonethiazole **7d** (6 × MIC) against *P. aeruginosa*.

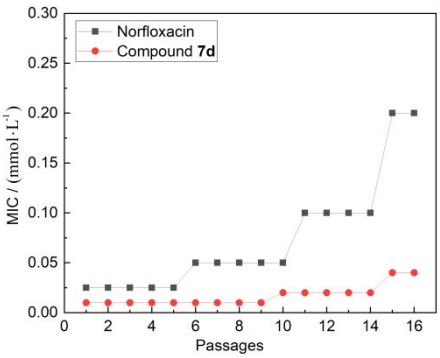

Figure 5 Bacterial resistance test for quinazolonethiazole **7d** towards the *P. aeruginosa*.

showed that susceptibility of *P. aeruginosa* nearly was unaffected even after 9 passages, followed by slower resistant development compared to the clinical drug norfloxacin. This information indicated that quinazolonethiazole **7d** with low bacterial resistance might have future potential for further development as antibacterial agent.

Cytotoxicity

Cytotoxicity is one of the most decisive factors in determining the fate of potential candidate molecules. Thiazole may undergo hepatotoxicity due to multi-step bioactivation to generate thioamides.[25] So the cell viability of LO2 cell (normal hepatocyte cell) was measured in the presence of highly active compound **7d** by MTT assay. The result in Figure 6 demonstrated that the LO2 cell viability treated by quinazolonethiazole **7d** remained around 100% at 0.01 mmol/L (concentration at which **7d** showed good inhibition against *P. aeruginosa*), while compound **7d** displayed low toxicity at 4 × MIC value. This manifested that quinazolonethiazole **7d** had no significant effect on the mammalian cell when inhibiting the growth of *P. aeruginosa*.

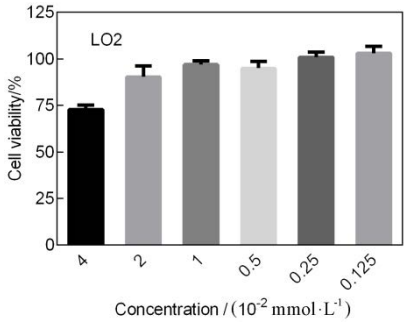

Figure 6 Cell viability of hexyl oxime derivative **7d** in LO2 cell.

ADME study

The failures to develop many clinical candidates are attributed to poor pharmacokinetics and bioavailability in addition to efficacy and toxicity.[26] To better understand the pharmacokinetics and bioavailability of quinazolonethiazole **7d**, the ADME study was performed using online software SwissADME. The Lipinski rule is widely used in drug design and development on account of its important determinants in assessing the pharmacokinetic properties associated with oral bioavailability.[27] Table 2 showed that compound **7d** tended to have high oral bioavailability because it met the Lipinski rule and had the same oral bioavailability score with norfloxacin. Moreover, according to the Brain Or IntestinaL EstimateD permeation method, the predictive results pointed out that compound **7d** displayed high gastrointestinal tract (GI) absorption and could not penetrate blood-brain barrier (BBB). All the data suggested quinazolonethiazole **7d** *in silico* had excellent drug-likeness and appreciable pharmacokinetic profiles.

Table 2 The ADME data of quinazolonethiazole **7d**

	Quinazolonethiazole **7d**	Norfloxacin
MW (g/mol) < 500	404.91	319.33
Mlog *P* ≤ 4.15	2.21	1.04
H-bond acceptors < 10	5	4
H-bond donors < 5	0	2
Rotatable bonds < 10	9	3
Lipinski violations	0	0
Bioavailability Score	0.55	0.55
GI absorption	High	High
BBB permeant	No	No

Bacterial membrane permeabilization

Cell membranes can prevent antibiotics from entering bacteria or excrete antibiotics out of membrane to induce drug-resistance, so the development of membrane-targeted antimicrobial agents is expected to overcome bacterial resistance.[28] The estimation of membrane damage by quinazolonethiazole **7d** in different concentrations was performed with propidium iodide (PI), which is a common staining reagent that penetrates compromised membrane to produce fluorescence.[29] Figure 7 demonstrated the increase in fluorescence intensity of *P. aeruginosa* cells on treatment with increasing concentrations of compound **7d**, which further indicated the increased uptake of the dye by the membrane of compromised cells. The gradually increased number of red fluorescent cells under fluorescence microscopy provided additional support for the occurrence of bacterial membrane damage. In other words, quinazolonethiazole **7d** could damage the membrane of *P. aeruginosa* leading to cell death.

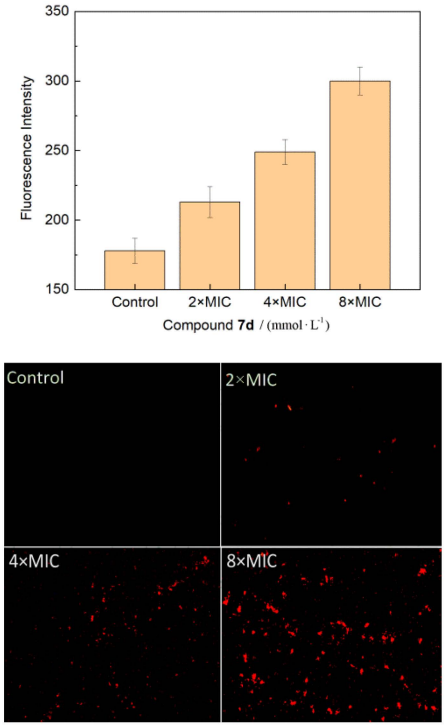

Figure 7 Estimation of membrane damage in *P. aeruginosa* treated with quinazolonethiazole **7d** by fluorescence and microscope.

Interaction of quinazolonethiazole 7d with topoisomerase IV and penicillin-binding protein (PBP)

In order to further provide appropriate antibacterial sights, the interactions between the highly bioactive molecule quinazolonethiazole **7d** and biomolecular enzymes topoisomerase IV or PBP (crystal data: protein data bank) were investigated by molecular docking.[30] Docking results for the topoisomerase IV (Figure 8A) demonstrated that the carbonyl group of quinazolone could form hydrogen bond with DC-3 of DNA at the distance of 2.3 Å. Noticeably, the nitrogen atom of imine fragment could bind with SER-79 residue through hydrogen bond, which further explained that the introduction of imine was beneficial to exert antibacterial activity. Besides, hydrogen bonds were formed between the carbonyl group of quinazolone and residue SER-485 of PBP, the oxygen atom of imine fragment and THR-487 residue (Figure 8B).

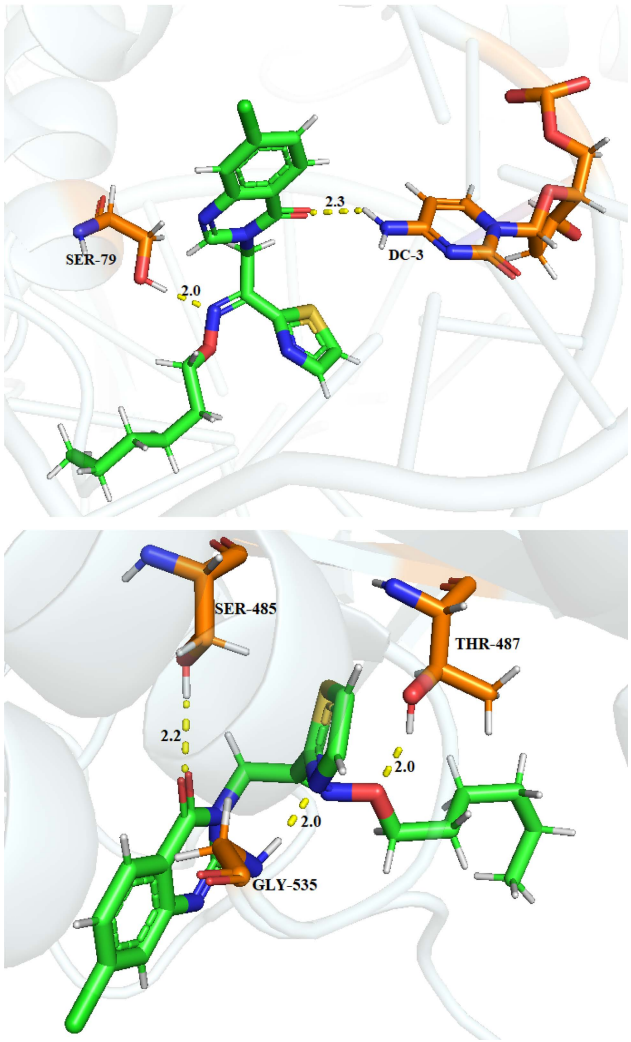

Figure 8 Interaction view of quinazolonethiazole **7d** in the binding site of (**A**) DNA topoisomerase IV (PDB code: 3RAF) and (**B**) PBP (PDB code: 6VJE), respectively.

Furthermore, the nitrogen atom of thiazole was involved in the hydrogen bond with glycine on PBP, which revealed the importance of thiazole in antibacterial. All hydrogen bonds were conducive to stabilizing the complexes between enzyme and quinazolonethiazole, which might further provide clues regarding good antibacterial effect of quinazolonthiazole.

Interaction of quinazolonethiazole 7d with DNA

As life-based biomacromolecule encoding genetic instructions, DNA is involved in the growth and development of organisms and also responsible for abnormality such as cancer and mutation.[31] Therefore, the study of the interaction between DNA and targeting compound can explain the action mechanism of some drugs, which is of great significance for finding antibacterial drugs with combating bacterial resistance, low cytotoxicity and good curative effect.[32] Calf thymus DNA is applied for DNA binding agent to perform *in vitro* interaction with quinazolonethiazole **7d**.

The ultraviolet-visible absorption in Figure 9 displayed that the absorbance peak of DNA (a constant concentration of 7.44×10^{-5} mol/L) progressively enhanced at 260 nm together with slightly blue shift as the proportionately improved concentration of **7d**. Meantime, the absorbance at 260 nm by adding up of quinazolonethiazole **7d** and free DNA was less than that of **7d**-DNA complex (inset of Figure 9). This proved a hyperchromic effect existing between DNA and **7d**, which might be due to DNA

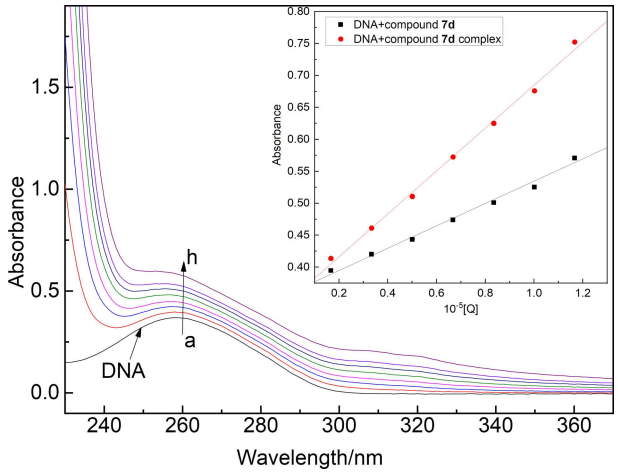

Figure 9 Interaction between DNA and different concentrations of **7d** (0—1.75×10^{-5} mol/L and in increment of 1.75×10^{-5} mol/L).

denaturation caused by interaction of DNA and molecule, leading to partial disintegration of DNA double helix and exposure of some DNA bases.[33-34] In a nutshell, the results suggested a strong interaction between DNA and quinazolonethiazole **7d**.

Competitive experiments of quinazolonethiazole 7d and AO with DNA

To illuminate the binding model of DNA and quinazolonethiazole **7d**, further investigation was carried out by the fluorescent probe of acridine orange (AO), a nucleic acid binding dye that could intercalate into DNA to emit fluorescence.[35] The fluorescence intensity of the DNA-AO system in Figure 10 gradually decreased at around 540 nm as the amount of quinazolonethiazole **7d** increased, indicating that quinazolonethiazole **7d** could effectively intercalate DNA by substituting AO to exert powerful bioactivity.

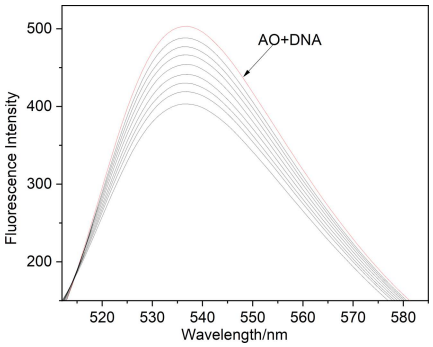

Figure 10 Competitive experiments between compound **7d** and AO with DNA.

Conclusions

A type of new quinazolonthiazoles was developed *via* several easy synthetic steps comprising cyclization, bromination, nucleophilic substitution and condensation from aminobenzoic acids, and their medicinal chemical biological assay revealed that some target quinazolonethiazoles enjoyed good antibacterial activity toward the tested strains. Particularly, the hexyl oxime derivative **7d** showed the best antimicrobial activity, and also exhibited stronger activity with MIC value of 0.01 mmol/L than the reference drugs chloramphenicol and norfloxacin against *P. aeruginosa*. The SAR in Figure 11 suggested that the presence of imine was

beneficial for inhibiting the growth of bacteria, which was also demonstrated by the docking study of quinazolonethiazole **7d** with topoisomerase IV. In addition, the highly active molecule **7d** with low hepatotoxicity might damage bacterial cell by enhancing the permeability of membrane and disturb bacterial growth by intercalating into DNA, rendering unapparent resistant tendency and bactericidal activity. The *in silico* ADME investigation also revealed that quinazolonethiazole **7d** possessed excellent drug-likeness and considerable pharmacokinetic profiles. These results provided helpful information for further optimization of quinazolonethiazole as potential therapeutics for infectious diseases caused by bacteria.

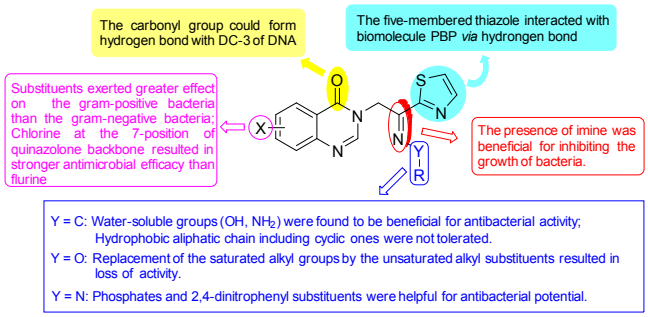

Figure 11 Brief biological summary of synthesized target quinazolonethiazoles.

Experimental

General methods. All purchased reagents and solvents were used directly without further purification. Melting points: X–6 melting point apparatus; TLC analysis: pre-coated silica gel plates; ^{1}H NMR and ^{13}C NMR spectra: AVANCE III 600 MHz spectrometer with tetramethylsilane (TMS) as reference. Coupling constants (*J*): hertz (Hz); Signals: singlet (s), doublet (d), triplet (t), quartet (q) as well as multiplet (m); Mass spectra: LCMS-2010A; High-resolution mass spectra (HRMS): IonSpec FTICR mass spectrometer with ESI resource. The compounds purity was determined to be >95% by HPLC (1 mL/min flow, 95%—60% linear gradient of solvent A (acetonitrile) in B (water) over 30 min).

Quinazolone (**2a—2d**): The synthesis of quinazolones **2a—2d** was done referring the reported literature.[36]

Quinazolonethiazole (**3a**): Compound **9** (8.81 g, 0.04 mol) and potassium carbonate (4.04 g, 0.03 mol) were added to acetonitrile with quinazolone **2a** (5.00 g, 0.03 mol). The mixture was stirred at 50 °C until the reaction was completed by TLC monitoring. The precipitated solid was filtered, washed with water and purified by silica gel column chromatography (eluent, dichloromethane/petroleum ether, 2/1, *V*/*V*) to afford desirable product **3a** (3.09 g) as yellow solid. Yield: 36.7%; m.p. 174—175 °C; Purity: 98%; ^{1}H NMR (600 MHz, DMSO-d_6) δ: 8.45 (s, 1H, quinazolinone-2-*H*), 8.38 (d, *J* =3.0 Hz, 1H, thiazole-4-*H*), 8.29 (d, *J* = 3.0 Hz, 1H, thiazole-5-*H*), 8.15 (d, *J* = 8.5 Hz, 1H, quinazolinone-5-*H*), 7.83 (d, *J* = 1.9 Hz, 1H, quinazolinone-8-*H*), 7.63 (dd, *J* = 8.5, 2.0 Hz, 1H, quinazolinone-6-*H*), 5.67 (s, 2H, CH_2); ^{13}C NMR (151 MHz, DMSO-d_6) δ: 186.58 (CH_2CO), 163.97 (quinazolinone-4-*C*), 160.03, 150.11, 149.62, 146.03, 139.84, 129.41, 128.65, 128.14, 127.04, 120.60, 52.50 (CH_2); HRMS (ESI) calcd. for $C_{13}H_8ClN_3O_2S$ $[M+H]^+$, 306.0104; found, 306.0100.

Quinazolonethiazole (**3b**): Yellow solid. Yield: 25.2%; m.p. 174—175 °C; Purity: 99%; ^{1}H NMR (600 MHz, DMSO-d_6) δ: 8.45 (s, 1H, quinazolinone-2-*H*), 8.38 (d, *J* = 2.8 Hz, 1H, thiazole-4-*H*), 8.29 (d, *J* = 2.9 Hz, 1H, thiazole-5-*H*), 8.22 (dd, *J* = 8.7, 6.3 Hz, 1H, quinazolinone-5-*H*), 7.55 (dd, *J* = 9.9, 1.9 Hz, 1H, quinazolinone-8-*H*) 7.46 (td, *J* = 8.6, 2.1 Hz, 1H, quinazolinone-6-*H*), 5.67 (s, 2H, CH_2); ^{13}C NMR (151 MHz, DMSO-d_6) δ: 186.65, 167.09, 165.42, 163.98, 159.92, 150.77, 150.69, 150.05, 146.03, 129.79, 129.71, 129.40, 118.83, 116.51, 116.35, 113.10, 112.95, 52.43; HRMS (ESI) calcd. for $C_{13}H_8FN_3O_2S$ $[M+H]^+$, 290.0400; found, 290.0393.

Quinazolonthiazole (**3c**): Yellow solid. Yield: 49.9%; m.p. 214—215 °C; Purity: 99%; ^{1}H NMR (600 MHz, DMSO-d_6) δ: 8.84 (d, *J* = 2.0 Hz, 1H, quinazolinone-5-*H*), 8.64—8.59 (m, 2H, quinazolinone-2-*H*, quinazolinone-7-*H*), 8.40 (d, *J* = 2.6 Hz, 1H, thiazole-4-*H*), 8.30 (d, *J* = 2.7 Hz, 1H, thiazole-5-*H*), 7.97 (d, *J* = 8.9 Hz, 1H, quinazolinone-8-*H*), 5.73 (s, 2H, CH_2); ^{13}C NMR (151 MHz, DMSO-d_6) δ: 186.25 (CH_2CO), 163.83 (quinazolinone-4-*C*), 159.91, 152.54, 151.89, 146.08, 146.01, 129.80, 129.53, 129.18, 122.65, 121.81, 52.74 (CH_2); HRMS (ESI) calcd. for $C_{13}H_8N_4O_4S$ $[M+H]^+$, 317.0345; found, 317.0340.

Quinazolonthiazole (**3d**): Yellow solid. Yield: 40.8%; m.p. 227—231 °C; Purity: 99%; ^{1}H NMR (600 MHz, DMSO-d_6) δ: 8.55 (s, 1H, quinazolinone-2-*H*), 8.39 (d, *J* = 2.8 Hz, 1H, thiazole-4-*H*), 8.30 (d, *J* = 2.8 Hz, 1H, thiazole-5-*H*), 8.21 (d, *J* = 1.9 Hz, 1H, quinazolinone-7-*H*), 8.07 (d, *J* = 1.8 Hz, 1H, quinazolinone-5-*H*), 5.70 (s, 2H, CH_2); ^{13}C NMR (151 MHz, DMSO-d_6) δ: 186.25, 163.85, 159.18, 149.90, 146.07, 143.97, 134.93, 133.02, 131.93, 129.49, 124.85, 124.06, 52.75; HRMS (ESI) calcd. for $C_{13}H_7Cl_2N_3O_2S$ $[M+H]^+$, 339.9714; found, 339.9707

Compound (**4a**): Intermediate **3a** (100 mg, 0.33 mmol) and propylamine (39 mg, 0.66 mmol) in ethanol were condensed with acetic acid as catalyst at 80 °C. After the reaction was accomplished (monitored by TLC), the precipitated solid was filtered off, washed with ice water and recrystallized from ethanol to afford target compound **4a** (46 mg) as white solid. Yield: 40.7%; m.p. 200—201 °C; Purity: 97%; ^{1}H NMR (600 MHz, $CDCl_3$) δ: 8.59 (s, 1H, quinazolinone-2-*H*), 8.18 (d, *J* = 8.6 Hz, 1H, quinazolinone-5-*H*), 7.80 (d, *J* = 3.1 Hz, 1H, thiazole-4-*H*), 7.67 (d, *J* = 1.4 Hz, 1H, quinazolinone-8-*H*), 7.42 (dd, *J* = 8.6, 1.6 Hz, 1H, quinazolinone-6-*H*), 7.33 (d, *J* = 3.1 Hz, 1H, thiazole-5-*H*), 5.19 (s, 2H, CH_2), 3.91 (t, *J* = 6.9 Hz, 2H, $CH_2CH_2CH_3$), 1.83—1.76 (m, 2H, $CH_2CH_2CH_3$), 1.03 (t, *J* = 7.4 Hz, 3H, $CH_2CH_2CH_3$); ^{13}C NMR (151 MHz, $CDCl_3$) δ: 169.55 (*C*=N), 160.28 (quinazolinone-4-*C*), 154.79 (aromatic *C*), 149.32, 148.91, 143.34, 140.63, 128.15, 127.87, 127.07, 122.41, 120.29, 54.27, 42.08, 24.08, 12.01 (CH_3); HRMS (ESI) calcd. for $C_{16}H_{15}ClN_4OS$ $[M+H]^+$, 347.0733; found, 347.0723.

Compound (**4b**): White solid. Yield: 39.5%; m.p. 190—191 °C; Purity: 95%; ^{1}H NMR (600 MHz, $CDCl_3$) δ: 8.23 (d, *J* = 8.5 Hz, 1H, quinazolinone-5-*H*), 8.03 (s, 1H, quinazolinone-2-*H*), 7.80 (d, *J* = 3.2 Hz, 1H, thiazole-4-*H*), 7.68 (d, *J* = 1.5 Hz, 1H, quinazolinone-8-*H*), 7.45 (dd, *J* = 8.5, 1.7 Hz, 1H, quinazolinone-6-*H*), 7.27 (d, *J* = 3.3 Hz, 1H, thiazole-5-*H*), 4.52 (s, 2H, CH_2), 3.05 (s, 2H, NH_2), 2.97 (dd, *J* = 10.1, 5.2 Hz, 2H, CH_2NH_2), 2.89 (dd, *J* = 10.1, 5.3 Hz, 2H, $CH_2CH_2NH_2$); ^{13}C NMR (151 MHz, $CDCl_3$) δ: 177.63 (*C*=N), 162.20 (quinazolinone-4-*C*), 149.09, 144.05, 140.82, 128.37, 127.83, 127.11, 120.85, 120.08, 81.85, 53.75 (CH_2), 46.67; HRMS (ESI) calcd. for $C_{14}H_{15}ClN_5O_4S$ $[M+H]^+$, 348.0686; found, 348.0678.

Compound (**4c**): White solid. Yield: 35.2%; m.p. 190—191 °C; Purity: 99%; ^{1}H NMR (600 MHz, $CDCl_3$) δ: 8.23 (d, *J* = 8.5 Hz, 1H, quinazolinone-5-*H*), 8.12 (s, 1H, quinazolinone-2-*H*), 7.85 (d, *J* = 2.4 Hz, 1H, thiazole-4-*H*), 7.70 (s, 1H, quinazolinone-8-*H*), 7.46 (d, *J* = 8.5 Hz, 1H, quinazolinone-6-*H*), 7.33 (d, *J* = 2.4 Hz, 1H, thiazole-5-*H*), 4.83 (d, *J* = 14.3 Hz, 1H, CH_2), 4.46 (d, *J* = 14.3 Hz, 1H, CH_2), 3.91 (dd, *J* = 12.7, 6.5 Hz, 1H, CH_2OH), 3.73 (dd, *J* = 13.8, 6.8 Hz, 1H, CH_2OH), 3.49 (s, 1H, *OH*), 3.14 (d, *J* = 4.8 Hz, 2H, CH_2CH_2OH); ^{13}C NMR (151 MHz, $CDCl_3$) δ: 172.80, 161.80, 149.09, 148.89, 144.30, 140.99, 128.57, 128.07, 127.28, 120.98, 120.32, 96.07, 67.72, 51.33, 46.20; HRMS (ESI) calcd. for $C_{15}H_{13}ClN_4O_2S$ $[M+H]^+$, 349.0526; found, 349.0528.

Compound (**4d**): White solid. Yield: 58.0%; m.p. 189—193 °C; Purity: 99%; ^{1}H NMR (600 MHz, $CDCl_3$) δ: 8.61 (s, 1H, quinazolinone-2-*H*), 8.21 (d, *J* = 8.6 Hz, 1H, quinazolinone-5-*H*), 7.81 (d, *J* = 3.1 Hz, 1H, thiazole-4-*H*), 7.67 (d, *J* = 1.4 Hz, 1H, quinazolinone-8-*H*), 7.45—7.41 (m, 1H, quinazolinone-6-*H*), 7.31 (d, *J* = 3.1 Hz, 1H,

thiazole-5-*H*), 5.38 (s, 2H, CH_2), 3.78—3.73 (m, 1H, C*H*), 1.15—1.10 (m, 2H, cyclopropylimino-CH_2), 1.07 (d, *J* = 2.9 Hz, 2H, cyclopropylimino-CH_2); ^{13}C NMR (151 MHz, $CDCl_3$) *δ*: 169.94 (*C*=N), 160.41 (quinazolinone-4-*C*), 153.80, 148.98, 143.38, 140.74, 128.37, 128.00, 127.19, 122.12, 120.48, 50.92, 41.64, 35.59, 11.37; HRMS (ESI) calcd. for $C_{16}H_{13}ClN_4OS$ $[M+H]^+$, 345.0577; found, 345.0574.

Compound (**4e**): White solid. Yield: 32.8%; m.p. 193—196 °C; Purity: 99%; ^{1}H NMR (600 MHz, $CDCl_3$) *δ*: 8.61 (s, 1H, quinazolinone-2-*H*), 8.21 (d, *J* = 8.6 Hz, 1H, quinazolinone-5-*H*), 7.81 (d, *J* = 3.1 Hz, 1H, thiazole-4-*H*), 7.67 (d, *J* = 1.4 Hz, 1H, quinazolinone-8-*H*), 7.45—7.41 (m, 1H, quinazolinone-6-*H*), 7.31 (d, *J* = 3.1 Hz, 1H, thiazole-5-*H*), 5.38 (s, 2H, CH_2), 3.78—3.73 (m, 1H, C*H*), 1.15—1.10 (m, 2H, cyclopropylimino-CH_2), 1.07 (d, *J* = 2.9 Hz, 2H, cyclopropylimino-CH_2); ^{13}C NMR (151 MHz, $CDCl_3$) *δ*: 170.01, 160.16, 152.83, 149.08, 148.86, 143.25, 140.59, 128.16, 127.85, 127.05, 122.30, 120.33, 62.40, 50.79, 41.87, 34.90, 34.78, 24.95, 24.56; HRMS (ESI) calcd. for $C_{18}H_{17}ClN_4OS$ $[M+H]^+$, 373.0890; found, 373.0890.

Compound (**5a**): To a mixture of intermediate **3a** (100 mg, 0.33 mmol) and phenylhydrazine (71 mg, 0.66 mmol) in ethanol was added hydrochloric acid. The system was stirred at 80 °C until the reaction was completed (monitored by TLC, dichloromethane). The precipitated solid was filtered off, washed with ice water and ethanol to afford target compound (79 mg) as yellow solid. Yield: 61.0%; m.p. 228—229 °C; Purity: 98%; ^{1}H NMR (600 MHz, $CDCl_3$) *δ*: 13.31 (s, 1H, N*H*), 8.36 (s, 1H, quinazolinone-2-*H*), 8.25 (d, *J* = 8.5 Hz, 1H, quinazolinone-5-*H*), 7.99 (d, *J* = 3.1 Hz, 1H, thiazole-4-*H*), 7.72 (d, *J* = 1.5 Hz, 1H, quinazolinone-8-*H*), 7.45 (dd, *J* = 8.5, 1.6 Hz, 1H, quinazolinone-6-*H*), 7.38 (d, *J* = 3.2 Hz, 1H, thiazole-5-*H*), 7.29—7.26 (m, 2H, Ph-3,5-*H*), 7.16 (d, *J* = 8.0 Hz, 2H, Ph-2,6-*H*), 6.94 (t, *J* = 7.2 Hz, 1H, Ph-4-*H*), 5.27 (s, 2H, CH_2); ^{13}C NMR (151 MHz, $CDCl_3$) *δ*: 161.19, 160.50, 149.20, 147.68, 143.62, 143.24, 140.78, 129.49, 128.56, 128.08, 127.34, 124.44, 122.11, 120.63, 118.65, 113.97, 48.46; HRMS (ESI) calcd. for $C_{19}H_{14}ClN_5OS$ $[M+H]^+$, 396.0686; found, 396.0686.

Compound (**5b**): Yellow solid. Yield: 60.7%; m.p. > 250 °C; Purity: 98%; ^{1}H NMR (600 MHz, DMSO-d_6) *δ*: 12.39 (s, 1H, N*H*), 8.96 (d, *J* = 2.4 Hz, 1H, (2,4-dinitrophenyl)hydrazineylidene-3-*H*), 8.81 (s, 1H, quinazolinone-2-*H*), 8.56 (dd, *J* = 9.4, 2.3 Hz, 1H, (2,4-dinitrophenyl)hydrazineylidene-5-*H*), 8.13 (d, *J* = 8.6 Hz, 1H, (2,4-dinitrophenyl)hydrazineylidene-6-*H*), 8.01—7.98 (m, 2H, quinazolinone-5-*H*, thiazole-4-*H*), 7.88 (d, *J* = 3.0 Hz, 1H, quinazolinone-6-*H*), 7.78 (s, 1H, quinazolinone-8-*H*), 7.58 (d, *J* = 8.6 Hz, 1H, thiazole-5-*H*), 5.38 (s, 2H, CH_2). HRMS (ESI) calcd. for $C_{19}H_{12}ClN_7O_5S$ $[M+H]^+$, 486.0387; found, 486.0379.

Compound (**5c**): Yellow solid. Yield: 82.7%. m.p. > 250 °C; Purity: 97%; ^{1}H NMR (600 MHz, DMSO-d_6) *δ*: 12.22 (s, 1H, N*H*), 8.88 (s, 2H, isonicotinohydrazide-2,6-*H*), 8.78 (s, 1H, quinazolinone-2-*H*), 8.18 (d, *J* = 8.2 Hz, 1H, quinazolinone-5-*H*), 7.98 (s, 3H, isonicotinohydrazide-3,5-*H*, quinazolinone-8-*H*), 7.85 (s, 1H, thiazole-4-*H*), 7.77 (s, 1H, quinazolinone-6-*H*), 7.60 (d, *J* = 8.5 Hz, 1H, thiazole-5-*H*), 5.52 (s, 2H, CH_2). HRMS (ESI) calcd. for $C_{19}H_{13}ClN_6O_2S$ $[M+H]^+$, 425.0587; found, 425.0593.

Compound (**5d**): White solid. Yield: 56.3%; m.p. 223—225 °C; Purity: 99%; ^{1}H NMR (600 MHz, DMSO-d_6) *δ*: 12.20 (d, *J* = 36.5 Hz, 1H, N*H*), 8.54 (s, 1H, quinazolinone-2-*H*), 8.22 (d, *J* = 2.6 Hz, 1H, quinazolinone-5-*H*), 8.19 (d, *J* = 8.5 Hz, 1H, thiazole-4-*H*), 8.16 (d, *J* = 2.7 Hz, 1H, thiazole-5-*H*), 7.87 (s, 1H, quinazolinone-8-*H*), 7.63 (d, *J* = 8.5 Hz, 1H, quinazolinone-6-*H*), 7.26 (t, *J* = 7.6 Hz, 4H, diphenyl-3,5-*H*), 7.17 (t, *J* = 7.3 Hz, 2H, diphenyl-4-*H*), 6.95 (d, *J* = 7.8 Hz, 4H, diphenyl-2,6-*H*), 5.36 (s, 2H, CH_2); ^{13}C NMR (151 MHz, DMSO-d_6) *δ*: 159.47, 158.72, 149.77, 149.52, 149.48, 149.16, 143.40, 139.24, 129.74, 128.22, 127.48, 126.52, 125.41, 122.82, 120.34, 120.14, 120.11, 47.63; HRMS (ESI) calcd. for $C_{25}H_{19}ClN_5O_4S$ $[M+H]^+$, 552.0662; found, 552.0656.

Compound (**5e**): To a mixture of intermediate **3a** (100 mg, 0.33 mmol) and diphenyl hydrazinylphosphonate (165 mg, 0.66 mmol) in ethanol was added sodium acetate (53 mg, 0.66 mmol). The system was stirred at 80 °C until the reaction was completed (monitored by TLC, dichloromethane). The precipitated solid was filtered off, washed with ice water and ethanol to afford target compound (112 mg) as white solid. Yield: 71.3%; m.p. 234—235 °C; Purity: 96%; ^{1}H NMR (600 MHz, DMSO-d_6) *δ*: 11.38 (d, *J* = 26.9 Hz, 1H, N*H*), 8.37 (s, 1H, quinazolinone-2-*H*), 8.16 (d, *J* = 8.5 Hz, 1H, quinazolinone-5-*H*), 8.05 (d, *J* = 3.1 Hz, 1H, thiazole-4-*H*), 7.85 (d, *J* = 3.1 Hz, 1H, thiazole-5-*H*), 7.79 (d, *J* = 1.5 Hz, 1H, quinazolinone-8-*H*), 7.61 (dd, *J* = 8.5, 1.7 Hz, 1H, quinazolinone-6-*H*), 6.98 (t, *J* = 7.7 Hz, 2H, phenyl-3,5-*H*), 6.92 (d, *J* = 7.8 Hz, 2H, phenyl-2,6-*H*), 6.80 (t, *J* = 7.1 Hz, 1H, phenyl-4-*H*), 5.16 (s, 2H, CH_2); ^{13}C NMR (151 MHz, DMSO-d_6) *δ*: 160.14, 159.39, 153.84, 148.95, 142.89, 139.03, 128.36, 128.29, 127.33, 126.41, 126.30, 121.44, 120.31, 120.28, 119.74, 48.53; HRMS (ESI) calcd. for $C_{14}H_{15}ClN_5O_4S$ $[M+H]^+$, 476.0349; found, 476.0345.

Compound (**6**): White solid. Yield: 76.3%; m.p. > 250 °C; Purity: 98%; ^{1}H NMR (600 MHz, DMSO-d_6) *δ*: 12.87 (s, 1H, O*H*), 8.55 (s, 1H, quinazolinone-2-*H*), 8.15 (d, *J* = 8.4 Hz, 1H, quinazolinone-5-*H*), 8.13 (d, *J* = 3.2 Hz, 1H, thiazole-4-*H*), 8.09—8.07 (m, 1H, thiazole-5-*H*), 7.77 (s, 1H, quinazolinone-8-*H*), 7.59 (dd, *J* = 8.5, 2.0 Hz, 1H, quinazolinone-6-*H*), 5.47 (s, 2H, CH_2); ^{13}C NMR (151 MHz, DMSO-d_6) *δ*: 163.69, 159.99, 153.23, 150.73, 144.37, 142.75, 139.58, 128.65, 127.89, 126.85, 124.98, 120.92, 46.82; HRMS (ESI) calcd. for $C_{13}H_9ClN_4O_2S$ $[M+H]^+$, 321.0213; found, 321.0204.

Compound (**7a**): Compound **6** (200 mg, 0.62 mmol) and potassium carbonate (171 mg, 1.24 mmol) were stirred in acetonitrile at 50 °C for 0.5 h, then cooled to room temperature for adding methyl iodide (176 mg, 1.24 mmol) and continued to reaction at 50 °C. After the reaction was completed (monitored by TLC, dichloromethane), acetonitrile was removed and the residue was extracted with ethyl acetate (3 × 20 mL), dried over anhydrous sodium sulfate and purified by silica gel column chromatography (eluent, dichloromethane/petroleum ether, 2/1, *V*/*V*) to afford desirable product (137 mg) as white solid. Yield: 65.6%; m.p. 177—178 °C; Purity: 97%; ^{1}H NMR (600 MHz, DMSO-d_6) *δ*: 8.55 (s, 1H, quinazolinone-2-*H*), 8.15 (d, *J* = 7.9 Hz, 3H, quinazolinone-5-*H*, thiazole-4-*H*, thiazole-5-*H*), 7.79 (s, 1H, quinazolinone-8-*H*), 7.60 (d, *J* = 8.5 Hz, 1H, quinazolinone-6-*H*), 5.47 (s, 2H, CH_2), 3.95 (s, 3H, CH_3); ^{13}C NMR (151 MHz, DMSO-d_6) *δ*: 159.38, 152.37, 150.07, 149.01, 144.65, 142.58, 139.08, 128.18, 127.33, 126.38, 125.28, 120.26, 63.12, 46.16; HRMS (ESI) calcd. for $C_{14}H_{11}ClN_4O_2S$ $[M+H]^+$, 335.0369; found, 335.0363.

Compound (**7b**): White solid. Yield: 74.5%; m.p. 153—154 °C; Purity: 99%; ^{1}H NMR (600 MHz, $CDCl_3$) *δ*: 8.34 (s, 1H, quinazolinone-2-*H*), 8.26 (d, *J* = 5.7 Hz, 1H, quinazolinone-5-*H*), 7.99 (d, *J* = 3.2 Hz, 1H, thiazole-4-*H*), 7.70 (d, *J* = 1.9 Hz, 1H, quinazolinone-8-*H*), 7.59 (d, *J* = 3.2 Hz, 1H, thiazole-5-*H*), 7.43 (dd, *J* = 3.6, 2.0 Hz, 1H, quinazolinone-6-*H*), 5.45 (s, 2H, CH_2), 4.36 (q, *J* = 7.1 Hz, 2H, OCH_2), 1.36 (t, *J* = 7.1 Hz, 3H, CH_3); ^{13}C NMR (151 MHz, $CDCl_3$) *δ*: 160.33, 153.40, 148.76, 144.05, 143.33, 142.42, 140.45, 128.41, 127.80, 127.73, 126.93, 123.51, 120.68, 71.99, 46.86, 14.50; HRMS (ESI) calcd. for $C_{15}H_{14}ClN_4O_2S$ $[M+H]^+$, 349.0526; found, 349.05203.

Compound (**7c**): White solid. Yield: 54.0%; m.p. 172—173 °C; Purity: 96%; ^{1}H NMR (600 MHz, $CDCl_3$) *δ*: 8.26 (s, 1H, quinazolinone-2-*H*), 8.21 (d, *J* = 8.6 Hz, 1H, quinazolinone-5-*H*), 7.85 (d, *J* = 3.0 Hz, 1H, quinazolinone-8-*H*), 7.70 (d, *J* = 1.5 Hz, 1H, thiazole-4-*H*), 7.44 (dd, *J* = 8.6, 1.7 Hz, 1H, quinazolinone-6-*H*), 7.33 (d, *J* = 3.2 Hz, 1H, thiazole-5-*H*), 5.35 (s, 2H, CH_2), 4.27 (t, *J* = 6.6 Hz, 2H, OCH_2), 1.68—1.62 (m, 2H, OCH_2CH_2), 1.50—1.42 (m, 2H, OCH$_2$CH_2CH_2), 0.88 (t, *J* = 7.4 Hz, 3H, CH_3); ^{13}C NMR (151 MHz, $CDCl_3$) *δ*: 162.74, 160.10, 148.83, 148.79, 148.53, 147.58, 143.31, 140.49, 128.25, 128.13, 128.06, 127.82, 126.91, 126.88, 120.57, 76.08, 50.78, 31.00, 30.74, 18.91, 13.68; HRMS (ESI) calcd. for $C_{17}H_{17}ClN_4O_2S$ $[M+H]^+$, 377.0839; found, 377.0839.

Compound (**7d**): White solid. Yield: 79.7%; m.p. 172—173 °C; Purity: 99%; ^{1}H NMR (600 MHz, $CDCl_3$) δ: 8.33 (s, 1H, quinazolinone-2-*H*), 8.25 (d, *J* = 2.8 Hz, 1H, quinazolinone-5-*H*), 7.99 (d, *J* = 3.2 Hz, 1H, thiazole-4-*H*), 7.70 (d, *J* = 1.8 Hz, 1H, quinazolinone-8-*H*), 7.59 (d, *J* = 3.2 Hz, 1H, thiazole-5-*H*), 7.44—7.41 (m, 1H, quinazolinone-6-*H*), 5.45 (s, 2H, CH_2), 4.31 (t, *J* = 6.6 Hz, 2H, OCH_2), 1.75—1.70 (m, 2H, OCH$_2$CH_2), 1.39 (dd, *J* = 10.3, 4.5 Hz, 2H, OCH$_2$CH$_2$CH_2), 1.28 (dd, *J* = 7.1, 3.5 Hz, 4H, OCH$_2$CH$_2$CH$_2$CH_2CH_2), 0.86 (t, *J* = 6.9 Hz, 3H, CH_3); ^{13}C NMR (151 MHz, $CDCl_3$) δ: 159.93, 159.86, 152.96, 150.63, 149.58, 144.75, 143.14, 139.58, 128.70, 127.83, 127.80, 126.91, 126.81, 125.71, 120.81, 75.97, 46.73, 31.26, 28.87, 25.45, 22.29, 14.26; HRMS (ESI) calcd. for $C_{19}H_{21}ClN_4O_2S$ $[M+H]^+$, 405.1152; found, 405.1145.

Compound (**7e**): Yellow solid. Yield: 63.0%; m.p. 177—178 °C; Purity: 99%; ^{1}H NMR (600 MHz, DMSO-d_6) δ: 8.54 (s, 1H, quinazolinone-2-*H*), 8.19 (d, *J* = 3.2 Hz, 1H, quinazolinone-5-*H*), 8.18 (d, *J* = 3.2 Hz, 1H, thiazole-4-*H*), 8.15 (d, *J* = 8.5 Hz, 1H, quinazolinone-8-*H*), 7.78 (d, *J* = 1.9 Hz, 1H, thiazole-5-*H*), 7.60 (dd, *J* = 8.5, 2.0 Hz, 1H, quinazolinone-6-*H*), 5.50 (s, 2H, CH_2), 4.84 (d, *J* = 2.3 Hz, 2H, OCH_2), 3.53 (t, *J* = 2.2 Hz, 1H, C*H*). ^{13}C NMR (151 MHz, DMSO-d_6) δ: 174.75 (*C*=N), 162.93 (s, quinazolinone-4-C), 150.51 (aromatic *C*), 142.97, 138.00, 130.30, 120.34, 117.84 (C≡*C*H), 114.04 (*C*≡CH), 69.89 (OCH_2), 60.76 (*C*H_2). HRMS (ESI) calcd. for $C_{16}H_{11}ClN_4O_2S$ $[M+H]^+$, 359.0369; found, 359.03662.

Compound (**7f**): Yellow solid. Yield: 56.6%; m.p. 178—179 °C; Purity: 99%; ^{1}H NMR (600 MHz, $CDCl_3$) δ: 8.33 (s, 1H, quinazolinone-2-*H*), 8.23 (d, *J* = 8.5 Hz, 1H, quinazolinone-5-*H*), 8.06 (d, *J* = 3.1 Hz, 1H, thiazole-4-*H*), 7.72 (d, *J* = 2.8 Hz, 2H, quinazolinone-8-*H*, thiazole-5-*H*), 7.45 (dd, *J* = 8.5, 1.8 Hz, 1H, quinazolinone-6-*H*), 5.49 (s, 2H, CH_2), 4.95 (s, 2H, OCH_2). ^{13}C NMR (151 MHz, $CDCl_3$) δ: 160.34 (*C*=N), 152.37, 148.43, 147.74, 143.72, 142.98, 140.69, 128.33, 127.93, 127.12, 125.08, 120.53, 114.69, 60.07, 46.97. HRMS (ESI) calcd. for $C_{15}H_{10}ClN_5O_2S$ $[M+H]^+$, 360.0322; found, 360.03198.

Compound (**7g**): White solid. Yield: 45.8%; m.p. 155—157 °C; Purity: 99%; ^{1}H NMR (600 MHz, $CDCl_3$) δ: 8.31 (s, 1H, quinazolinone-2-*H*), 8.24 (dd, *J* = 8.5, 4.0 Hz, 1H, quinazolinone-5-*H*), 7.99 (dd, *J* = 4.4, 2.4 Hz, 1H, thiazole-4-*H*), 7.71—7.68 (m, 1H, quinazolinone-8-*H*), 7.60 (t, *J* = 2.6 Hz, 1H, thiazole-5-*H*), 7.44—7.40 (m, 1H, quinazolinone-6-*H*), 6.03—5.96 (m, 1H, OCH$_2$C*H*), 5.45 (s, 2H, CH_2), 5.32—5.28 (m, 1H, OCH$_2$CH=CH_2), 5.22 (d, *J* = 9.2 Hz, 1H, OCH$_2$CH=CH_2), 4.79 (d, *J* = 5.0 Hz, 2H, OCH_2); ^{13}C NMR (151 MHz, $CDCl_3$) δ: 160.34, 153.27, 148.69, 144.51, 143.37, 142.49, 140.44, 132.76, 132.71, 128.39, 128.24, 127.79, 127.72, 126.96, 123.76, 120.69, 119.08, 118.94, 46.83, 30.87; HRMS (ESI) calcd. for $C_{16}H_{13}ClN_4O_2S$ $[M+H]^+$, 361.0526; found, 361.05298.

Supporting Information

The supporting information for this article is available on the WWW under https://doi.org/10.1002/cjoc.202000627.

Acknowledgement

This work was supported by the National Natural Science Foundation of China (Nos. 21971212 and 21672173), the Research Funds for the Central Universities (No. XDJK2020C031), the China Postdoctoral Science Foundation (No. 2019M653821XB), the Postdoctoral Science Foundation Project of Chongqing Science and Technology Bureau (No. cstc2019jcyj-bshX0124), and the Chongqing Special Foundation for Postdoctoral Research Proposal (No. XmT2018082).

References

[1] (a) Jansen, K. U.; Knirsch, C.; Anderson, A. S. The Role of Vaccines in Preventing Bacterial Antimicrobial Resistance. *Nat. Med.* **2018**, *24*, 10–19; (b) Brown, E. D.; Wright, G. D. Antibacterial Drug Discovery in the Resistance Era. *Nature* **2016**, *529*, 336–343.

[2] (a) Mc Carlie, S.; Boucher, C. E.; Bragg, R. R. Molecular Basis of Bacterial Disinfectant Resistance. *Drug Resist. Update* **2020**, *48*, 100672; (b) Gunawan, C.; Marquis, C. P.; Amal, R.; Sotiriou, G. A.; Rice, S. A.; Harry, E. J. Widespread and Indiscriminate Nanosilver Use: Genuine Potential for Microbial Resistance. *ACS Nano* **2017**, *11*, 3438–3445.

[3] (a) Over, B.; Wetzel, S.; Grütter, C.; Nakai, Y.; Renner, S.; Rauh, D.; Waldmann, H. Natural-product-derived Fragments for Fragment-Based Ligand Discovery. *Nat. Chem.* **2013**, *5*, 21–28; (b) Kshirsagar, U. A. Recent Developments in the Chemistry of Quinazolinone Alkaloids. *Org. Biomol. Chem.* **2015**, *13*, 9336–9352; (c) Wan, X.; Yang, T.; Cuesta, A.; Pang, X.; Balius, T. E.; Irwin, J. J.; Shoichet, B. K.; Taunton, J. Discovery of Lysine-targeted EIF4E Inhibitors Through Covalent Docking. *J. Am. Chem. Soc.* **2020**, *142*, 4960–4964.

[4] (a) Liu, X.; Fu, H.; Jiang, Y.; Zhao, Y. A Simple and Efficient Approach to Quinazolinones under Mild Copper-Catalyzed Conditions. *Angew. Chem. Int. Ed.* **2009**, *48*, 348–351; (b) Fitzgerald, C. E.; Patel, S. B.; Becker, J. W.; Cameron, P. M.; Zaller, D.; Pikounis, V. B.; O'Keefe, S. J.; Scapin, G. Structural Basis for p38α Map Kinase Quinazolinone and Pyridol-pyrimidine Inhibitor Specificity. *Nat. Struct. Mol. Biol.* **2003**, *10*, 764–769.

[5] (a) Atobe, M.; Nagami, T.; Muramatsu, S.; Ohno, T.; Kitagawa, M.; Suzuki, H.; Ishiguro, M.; Watanabe, A.; Kawanishi, M. Discovery of Novel Transient Receptor Potential Vanilloid 4 (Trpv4) Agonists as Regulators of Chondrogenic Differentiation: Identification of Quinazolin-4(3*H*)-Ones and *in Vivo* Studies on a Surgically Induced Rat Model of Osteoarthritis. *J. Med. Chem.* **2019**, *62*, 1468–1483; (b) Peng, X. M.; Peng, L. P.; Li, S.; Avula, S. R.; Kannekanti, V. K.; Zhang, S. L.; Tam, K. Y.; Zhou, C. H. Quinazolinone Azolyl Ethanols: Potential Lead Antimicrobial Agents with Dual Action Modes Targeting Methicillin-Resistant *Staphylococcus aureus* DNA. *Future Med. Chem.* **2016**, *8*, 1927–1940.

[6] (a) Qian, Y.; Allegretta, G.; Janardhanan, J.; Peng, Z.; Mahasenan, K. V.; Lastochkin, E.; Gozun, M. M. N.; Tejera, S.; Schroeder, V. A.; Wolter, W. R.; Feltzer, R.; Mobashery, S.; Chang, M. Exploration of the Structural Space in 4(3*H*)-Quinazolinone Antibacterials. *J. Med. Chem.* **2020**, *63*, 5287–5296; (b) Janardhanan, J.; Bouley, R.; Martinez-Caballero, S.; Peng, Z. H.; Batuecas-Mordillo, M.; Meisel, J. E.; Ding, D. R.; Schroeder, V. A.; Wolter, W. R.; Mahasenan, K. V.; Hermoso, J. A.; Mobashery, S.; Chang, M. The Quinazolinone Allosteric Inhibitor of PBP 2a Synergizes with Piperacillin and Tazobactam Against Methicillin-resistant Staphylococcus aureus. *Antimicrob. Agents. Chemother.* **2019**, *63*, e02637-18.

[7] (a) Xiong, X.; Bromley, E. H. C.; Oelschlaeger, P.; Woolfson, D. N.; Spencer, J. Structural Insights into Quinolone Antibiotic Resistance Mediated by Pentapeptide Repeat Proteins: Conserved Surface Loops Direct the Activity of A QNR Protein from A Gram-negative Bacterium. *Nucleic Acids Res.* **2011**, *39*, 3917–3927; (b) Gao, W. W.; Zhou, C. H. Antimicrobial 2-aminothiazolyl Quinolones: What is Their Potential in the Clinic? *Future Med. Chem.* **2017**, *9*, 1461–1464.

[8] (a) Ceballos, S.; Kim, C.; Qian, Y. Y.; Mobashery, S.; Chang, M.; Torres, C. Susceptibility of Methicillin-Resistant Staphylococcus Aureus to Five Quinazolinone Antibacterials. *Antimicrob. Agents Chemother.* **2020**, *64*, e01344-19; (b) Rakesh, K. P.; Kumara, H. K.; Manukumar, H. M.; Gowda, D. C. Anticancer and DNA Binding Studies of Potential Amino Acids Based Quinazolinone Analogs: Synthesis, SAR and Molecular Docking. *Bioorg. Chem.* **2019**, *87*, 252–264.

[9] (a) Gatadi, S.; Lakshmi, T. V.; Nanduri, S. 4(3*H*)-Quinazolinone Derivatives: Promising Antibacterial Drug Leads. *Eur. J. Med. Chem.* **2019**, *170*, 157–172; (b) Peng, L. P.; Nagarajan, S.; Rasheed, S.; Zhou, C. H. Synthesis and Biological Evaluation of a New Class of Quinazolinoneazoles as Potential Antimicrobial Agents and Their Interactions with Calf Thymus DNA and Human Serum Albumin. *MedChemComm* **2015**, *6*, 222–229; (c) Shi, G.; He, X.; Shang, Y.; Yang, C.; Xiang, L. Oxidative

Rearrangement of Isatins with Arylamines Using H_2O_2 as Oxidant: A Facile Synthesis of Quinazoline-2,4-Diones and Evaluation of Their Antibacterial Activity. *Chin. J. Chem.* **2017**, *35*, 1835–1843.

[10] (a) Khatik, G. L.; Datusalia, A. K.; Ahsan, W.; Kaur, P.; Vyas, M.; Mittal, A.; Nayak, S. K. A Retrospect Study on Thiazole Derivatives as the Potential Antidiabetic Agents in Drug Discovery and Developments. *Curr. Drug. Discov. Technol.* **2018**, *15*, 163–177; (b) Zhang, H. Z.; He, S. C.; Peng, Y. J.; Zhang, H. J.; Gopala, L.; Tangadanchu, V. K. R.; Gan, L. L.; Zhou, C. H. Design, Synthesis and Antimicrobial Evaluation of Novel Benzimidazole-incorporated Sulfonamide Analogues. *Eur. J. Med. Chem.* **2017**, *136*, 165–183.

[11] (a) Wang, L. L.; Battini, N.; Bheemanaboina, R. R. Y.; Zhang, S. L.; Zhou, C. H. Design and Synthesis of Aminothiazolyl Norfloxacin Analogues as Potential Antimicrobial Agents and Their Biological Evaluation. *Eur. J. Med. Chem.* **2019**, *167*, 105–123; (b) Cui, S. F.; Wang, Y.; Lv, J. S.; Damu, G. L. V.; Zhou, C. H. Recent Advances in Application of Thiazole Compounds. *Sci. China Ser B-Chem.* **2012**, *42*, 1105–1131 (in Chinese); (c) Zhang, H. Z.; Gan, L. L.; Wang, H.; Zhou, C. H. New Progress in Azole Compounds as Antimicrobial Agents. *Mini-Rev. Med. Chem.* **2017**, *17*, 122–166.

[12] (a) Maddili, S. K.; Li, Z. Z.; Kannekanti, V. K.; Bheemanaboina, R. R. Y.; Tuniki, B.; Tangadanchu, V. K. R.; Zhou, C. H. Azoalkyl Ether Imidazo[2,1-B]Benzothiazoles as Potentially Antimicrobial Agents with Novel Structural Skeleton. *Bioorg. Med. Chem. Lett.* **2018**, *28*, 2426–2431; (b) Chen, Y. Y.; Gopala, L.; Bheemanaboina, R. R. Y.; Liu, H. B.; Cheng, Y.; Geng, R. X.; Zhou, C. H. Novel Naphthalimide Aminothiazoles as Potential Multitargeting Antimicrobial Agents. *ACS Med. Chem. Lett.* **2017**, *8*, 1331–1335; (c) Zhang, L.; Peng, X. M.; Damu, G. L. V.; Geng, R. X.; Zhou, C. H. Comprehensive Review in Current Developments of Imidazole-based Medicinal Chemistry. *Med. Res. Rev.* **2014**, *34*, 340–437.

[13] (a) Rouf, A.; Tanyeli, C. Bioactive Thiazole and Benzothiazole Derivatives. *Eur. J. Med. Chem.* **2015**, *97*, 911–927; (b) Cheng, Y.; Wang, H.; Addla, D.; Zhou, C. H. Current Researches and Applications of Azole-based Supermolecules as Medicinal Agents. *Chin. J. Org. Chem.* **2016**, *36*, 1–42; (c) Peng, X. M.; Damu, G. L. V.; Zhou, C. H. Current Developments of Coumarin Compounds in Medicinal Chemistry. *Curr. Pharm. Design* **2013**. *19*, 3884–3930.

[14] (a) Hou, X.; Zhang, J.; Zhao, X.; Chang, L.; Hu, P.; Liu, H. Design, Synthesis and Bioactivities Evaluation of Novel Quinazoline Analogs Containing Oxazole Units. *Chin. J. Chem.* **2014**, *32*, 538–544; (b) Damu, G. L. V.; Cui, S. F.; Peng, X. M.; Wen, Q. M.; Cai, G. X.; Zhou, C. H. Synthesis and bioactive Evaluation of a Novel Series of Coumarinazoles. *Bioorg. Med. Chem. Lett.* **2014**, *24*, 3605–3608; (c) Wang, X. L.; Wan, K.; Zhou, C. H. Synthesis of Novel Sulfanilamide-Derived 1,2,3-Triazoles and Their Evaluation for Antibacterial and Antifungal Activities. *Eur. J. Med. Chem.* **2010**, *45*, 4631–4639.

[15] (a) Cascioferro, S.; Carbone, D.; Parrino, B.; Pecoraro, C.; Giovannetti, E.; Cirrincione, G.; Diana, P. Therapeutic Strategies to Counteract Antibiotic Resistance in MRSA Biofilm-Associated Infections. *ChemMedChem* **2020**, *15,* 1–17; (b) Gao, W. W.; Gopala, L.; Bheemanaboina, R. R. Y.; Zhang, G. B.; Li, S.; Zhou, C. H. Discovery of 2-Aminothiazolyl Berberine Derivatives as Effectively Antibacterial Agents toward Clinically Drug-Resistant Gram-Negative Acinetobacter Baumanii. *Eur. J. Med. Chem.* **2018**, *146*, 15–37; (c) Mishra, I.; Mishra, R.; Mujwar, S.; Chandra, P.; Sachan, N. A Retrospect on Antimicrobial Potential of Thiazole Scaffold. *J. Heterocycl. Chem.* **2020**, *57*, 2304–2329.

[16] (a) Wang, L. L.; Battini, N.; Bheemanaboina, R. R. Y.; Ansari, M. F.; Chen, J. P.; Xie, Y. P.; Cai, G. X.; Zhang, S. L.; Zhou, C. H. A New Exploration Towards Aminothiazolquinolone Oximes as Potentially Multi-Targeting Antibacterial Agents: Design, Synthesis and Evaluation Acting on Microbes, DNA, HSA and Topoisomerase IV, *Eur. J. Med. Chem.* **2019**, *179*, 166–181; (b) Cui, S. F.; Addla, D.; Zhou, C. H. Novel 3-Aminothiazolquinolones: Design, Synthesis, Bioactive Evaluation, Sars, and Preliminary Antibacterial Mechanism. *J. Med. Chem.* **2016**, *59*, 4488–4510.

[17] (a) Nezhad-Mokhtari, P.; Ghorbani, M.; Roshangar, L.; Rad, J. S. A Review on the Construction of Hydrogel Scaffolds by Various Chemically Techniques for Tissue Engineering. *Eur. Polym. J.* **2019**, *117*, 64–76; (b) Zhou, C. H.; Wang, Y. Recent Researches in Triazole Compounds as Medicinal Drugs. *Curr. Med. Chem.* **2012**, *19*, 239–280; (c) Wang, L. Y.; Wu, S. M.; Tang, H.; Meier, H.; Cao, D. R. An Efficient Probe for Sensing Different Concentration Ranges of Glutathione Based on Aie-Active Schiff Base Nanoaggregates with Distinct Reaction Mechanism. *Sens. Actuators B*: *Chem.* **2018**, *273*, 1085–1090.

[18] (a) Liu, X.; Hamon, J. R. Recent Developments in Penta-, Hexa- and Heptadentate Schiff Base Ligands and Their Metal Complexes. *Coordin. Chem. Rev.* **2019**, *389*, 94–118; (b) Zhang, H. Z.; Zhao, Z. L.; Zhou, C. H. Recent Advance in Oxazole-Based Medicinal Chemistry. *Eur. J. Med. Chem.* **2018**, *144*, 444–492.

[19] (a) Ding, Y.; Li, Z.; Xu, C.; Qin, W.; Wu, Q.; Wang, X.; Cheng, X.; Li, L.; Huang, W. Fluorogenic Probes/Inhibitors of B-Lactamase and Their Applications in Drug-Resistant Bacteria. *Angew. Chem. Int. Ed.* **2020**, *59,* 2–19; (b) Cascioferro, S.; Parrino, B.; Carbone, D.; Schillaci, D.; Giovannetti, E.; Cirrincione, G.; Diana, P. Thiazoles, Their Benzofused Systems, and Thiazolidinone Derivatives: Versatile and Promising Tools to Combat Antibiotic Resistance. *J. Med. Chem.* **2020**, *63*, 7923–7956.

[20] (a) Hu, Y. Y.; Wang, J.; Li, T. J.; Bheemanaboina, R. R. Y.; Ansari, M. F.; Cheng, Y.; Zhou, C. H. An Unexpected Discovery toward Novel Membrane Active Sulfonyl Thiazoles as Potential MRSA DNA Intercalators. *Future Med. Chem.* **2020**, *12*, 1709–1727; (b) Shi, Y. A.; Zhou, C. H. Synthesis and Evaluation of a Class of New Coumarin Triazole Derivatives as Potential Antimicrobial Agents. *Bioorg. Med. Chem. Lett.* **2011**, *21*, 956–960.

[21] (a) Zhan, X.; Xu, Y.; Qi, Q.; Wang, Y.; Shi, H.; Mao, Z. Synthesis, Cytotoxic, and Antibacterial Evaluation of Quinazolinone Derivatives with Substituted Amino Moiety. *Biodiversity* **2018**, *15*, e1700513; (b) Hu, Y. Y.; Yadav Bheemanaboina, R. R.; Battini, N.; Zhou, C. H. Sulfonamide-Derived Four-Component Molecular Hybrids as Novel DNA-Targeting Membrane Active Potentiators against Clinical Escherichia Coli. *Mol. Pharm.* **2019**, *16*, 1036–1052; (c) Wang, X.; Yin, J.; Shi, L.; Zhang, G. P.; Song, B. Design, Synthesis, and Antibacterial Activity of Novel Schiff Base Derivatives of Quinazolin-4(3*H*)-one. *Eur. J. Med. Chem.* **2014**, *77*, 65–74.

[22] (a) Kim, W.; Zhu, W. P.; Hendricks, G. L.; Van Tyne, D.; Steele, A. D.; Keohane, C. E.; Fricke, N.; Conery, A. L.; Shen, S.; Pan, W.; Lee, K.; Rajamuthiah, R.; Fuchs, B. B.; Vlahovska, P. M.; Wuest, W. M.; Gilmore, M. S.; Gao, H. J.; Ausubel, F. M.; Mylonakis, E. A New Class of Synthetic Retinoid Antibiotics Effective against Bacterial Persisters. *Nature* **2018**, *556*, 103–107; (b) Zhang, Y.; Tangadanchu, V. K. R.; Cheng, Y.; Yang, R. G.; Lin, J. M.; Zhou, C. H. Potential Antimicrobial Isopropanol-Conjugated Carbazole Azoles as Dual Targeting Inhibitors of Enterococcus faecalis. *ACS Med. Chem. Lett.* **2018**, *9*, 244–249.

[23] (a) Pankey, G. A.; Sabath, L. D. Clinical Relevance of Bacteriostatic Versus Bactericidal Mechanisms of Action in the Treatment of Gram-Positive Bacterial Infections. *Clin. Infect. Dis.* **2004**, *38*, 864–870; (b) Wang, Y. N.; Bheemanaboina, R. R. Y.; Gao, W. W.; Kang, J.; Cai, G. X.; Zhou, C. H. Discovery of Benzimidazole-Quinolone Hybrids as New Cleaving Agents toward Drug-Resistant Pseudomonas Aeruginosa DNA. *ChemMedChem* **2018**, *13*, 1004–1017; (c) Sui, Y. F.; Li, D.; Wang, J.; Bheemanaboina, R. R. Y.; Ansari, M. F.; Gan, L. L.; Zhou, C. H. Design and Biological Evaluation of a Novel Type of Potential Multi-Targeting Antimicrobial Sulfanilamide Hybrids in Combination of Pyrimidine and Azoles. *Bioorg. Med. Chem. Lett*. **2020**, *30,* 126982.

[24] (a) Li, D.; Bheemanaboina, R. R. Y.; Battini, N.; Tangadanchu, V. K. R.; Fang, X. F.; Zhou, C. H. Novel Organophosphorus Aminopyrimidines as Unique Structural DNA-Targeting Membrane Active Inhibitors Towards Drug-Resistant Methicillin-Resistant Staphylococcus Aureus. *MedChemComm* **2018**, *9*, 1529–1537; (b) Lin, S. M.; Li, H. X.; Tao, Y. W.; Liu, J. Y.; Yuan, W. C.; Chen, Y. Z.; Liu, Y.; Liu, S. P. *In Vitro* and *in Vivo* Evaluation of Membrane-Active Flavone Amphiphiles: Semisyn-

thetic Kaempferol-Derived Antimicrobials against Drug-Resistant Gram-Positive Bacteria. *J. Med. Chem.* **2020**, *63*, 5797–5815.

[25] (a) Barnette, D. A.; Schleiff, M. A.; Osborn, L. R.; Flynn, N.; Matlock, M.; Swamidass, S. J.; Miller, G. P. Dual Mechanisms Suppress Meloxicam Bioactivation Relative to Sudoxicam. *Toxicology* **2020**, *440*, 152478; (b) Zhang, Y.; Tangadanchu, V. K. R.; Bheemanboina, R. R. Y.; Cheng, Y.; Zhou, C. H. Novel Carbazole-Triazole Conjugates as DNA-Targeting Membrane Active Potentiators against Clinical Isolated Fungi. *Eur. J. Med. Chem.* **2018**, *155*, 579–589; (c) Jeyakkumar, P.; Liu, H. B.; Gopala, L.; Cheng, Y.; Peng, X. M.; Geng, R. X.; Zhou, C. H. Novel Benzimidazolyl Tetrahydroprotoberberines: Design, Synthesis, Antimicrobial Evaluation and Multi-Targeting Exploration. *Bioorg. Med. Chem. Lett.* **2017**, *27*, 1737–1743.

[26] Cardoso, M. V. D.; de Oliveira, G. B.; de Siqueira, L. R. P.; Espindola, J. W. P.; da Silva, E. B.; Mendes, A. P. D.; Pereira, V. R. A.; de Castro, M. C. A. B.; Ferreira, R. S.; Villela, F. S.; da Costa, F. M. R.; Meira, C. S.; Moreira, D. R. M.; Soares, M. B. P.; Leite, A. C. L. 2-(Phenylthio)-Ethylidene Derivatives as Anti-Trypanosoma Cruzi Compounds: Structural Design, Synthesis and Antiparasitic Activity. *Eur. J. Med. Chem.* **2019**, *180*, 191–203.

[27] Daina, A.; Zoete, V. A Boiled-Egg to Predict Gastrointestinal Absorption and Brain Penetration of Small Molecules. *ChemMedChem* **2016**, *11*, 1117–1121.

[28] (a) Sun, H.; Ansari, M. F.; Battini, N.; Bheemanaboina, R. R. Y.; Zhou, C. H. Novel Potential Artificial MRSA DNA Intercalators: Synthesis and Biological Evaluation of Berberine-Derived Thiazolidinediones. *Org. Chem. Front.* **2019**, *6*, 319–334; (b) Kang, J.; Gopala, L.; Tangadanchu, V. K. R.; Gao, W. W.; Zhou, C. H. Novel Naphthalimide Nitroimidazoles as Multitargeting Antibacterial Agents against Resistant Acinetobacter Baumannii. *Future Med. Chem.* **2018**, *10*, 711–724.

[29] (a) Roy, S.; Mondal, A.; Yadav, V.; Sarkar, A.; Banerjee, R.; Sanpui, P.; Jaiswal, A. Mechanistic Insight into the Antibacterial Activity of Chitosan Exfoliated MOS_2 Nanosheets: Membrane Damage, Metabolic Inactivation, and Oxidative Stress. *ACS Appl. Bio. Mater.* **2019**, *2*, 2738–2755; (b) Wang, Y. N.; Bheemanaboina, R. R. Y.; Cai, G. X.; Zhou, C. H. Novel Purine Benzimidazoles as Antimicrobial Agents by Regulating ROS Generation and Targeting Clinically Resistant Staphylococcus Aureus DNA Groove. *Bioorg. Med. Chem. Lett.* **2018**, *28*, 1621–1628.

[30] (a) Gao, W. W.; Rasheed, S.; Tangadanchu, V.; Sun, Y.; Peng, X. M.; Cheng, Y.; Zhang, F. X.; Lin, J. M.; Zhou, C. H. Design, Synthesis and Biological Evaluation of Amino Organophosphorus Imidazoles as a New Type of Potential Antimicrobial Agents. *Sci. China Chem.* **2017**, *60*, 769–785; (b) Li, Z. Z.; Gopala, L.; Tangadanchu, V. K. R.; Gao, W. W.; Zhou, C. H. Discovery of Novel Nitroimidazole Enols as Pseudomonas aeruginosa DNA Cleavage Agents. *Bioorg. Med. Chem.* **2017**, *25*, 6511–6522.

[31] (a) Zhang, Y.; Damu, G. L. V.; Cui, S. F.; Mi, J. L.; Tangadanchu, V. K. R.; Zhou, C. H. Discovery of Potential Antifungal Triazoles: Design, Synthesis, Biological Evaluation, and Preliminary Antifungal Mechanism Exploration. *MedChemComm* **2017**, *8*, 1631–1639; (b) Hu, C. F.; Zhang, P. L.; Sui, Y. F.; Lv, J. S.; Ansari, M. F.; Battini, N.; Li, S.; Zhou, C. H.; Geng, R. X. Ethylenic Conjugated Coumarin Thiazolidinediones as New Efficient Antimicrobial Modulators against Clinical Methicillin-Resistant Staphylococcus aureus. *Bioorg. Chem.* **2020**, *94*. 103434.

[32] (a) Li, Z. Z.; Tangadanchu, V. K. R.; Battini, N.; Bheemanaboina, R. R. Y.; Zang, Z. L.; Zhang, S. L.; Zhou, C. H. Indole-Nitroimidazole Conjugates as Efficient Manipulators to Decrease the Genes Expression of Methicillin-Resistant Staphylococcus aureus. *Eur. J. Med. Chem.* **2019**, *179*, 723–735; (b) Fang, X. F.; Li, D.; Tangadanchu, V. K. R.; Gopala, L.; Gao, W. W.; Zhou, C. H. Novel Potentially Antifungal Hybrids of 5-Flucytosine and Fluconazole: Design, Synthesis and Bioactive Evaluation. *Bioorg. Med. Chem. Lett.* **2017**, *27*, 4964–4969.

[33] Liu, H. B.; Gao, W. W.; Tangadanchu, V. K. R.; Zhou, C. H.; Geng, R. X. Novel Aminopyrimidinyl Benzimidazoles as Potentially Antimicrobial Agents: Design, Synthesis and Biological Evaluation. *Eur. J. Med. Chem.* **2018**, *143*, 66–84.

[34] (a) Lauria, T.; Slator, C.; McKee, V.; Müller, M.; Stazzoni, S.; Crisp, A. L.; Carell, T.; Kellett, A. A Click Chemistry Approach to Developing Molecularly Targeted DNA Scissors. *Chem. Eur. J.* **2020**, *26*, 1–12; (b) Zhang, G. B.; Maddili, S. K.; Tangadanchu, V. K. R.; Gopala, L.; Gao, W. W.; Cai, G. X.; Zhou, C. H. Discovery of Natural Berberine-Derived Nitroimidazoles as Potentially Multi-Targeting Agents against Drug-Resistant Escherichia coli. *Sci. China Chem.* **2018**, *61*, 557–568.

[35] Zhang, G.; Ma, Y. Spectroscopic Studies on the Interaction of Sodium Benzoate, a Food Preservative, with Calf Thymus DNA. *Food Chem.* **2013**, *141*, 41–47.

[36] Cao, Q. C.; Wang, H.; Tangadanchu, V. K. R.; Gopala, L.; Cai, G. X.; Zhou, C. H. Design and Synthesis of Quinazolinone Imidazoles and Their Antibacterial and DNA-targeting Investigation. *Sci. Sin. Chim.* **2017**, *47*, 844–858 (in Chinese).

Manuscript received: November 15, 2020
Manuscript revised: December 17, 2020
Manuscript accepted: December 18, 2020
Accepted manuscript online: December 23, 2021

